Precise cross-section estimation on tubular organs

Florent Grélard[1,2], Fabien Baldacci[1,2], Anne Vialard[1,2], and Jacques-Olivier Lachaud[3]

[1] Univ. Bordeaux, LaBRI, UMR 5800, F-33400 Talence, France
[2] CNRS, LaBRI, UMR 5800, F-33400 Talence, France
[3] Université Savoie Mont Blanc, LAMA, UMR 5127, F-73376 France

Abstract. In this article we present a new method to estimate precisely the cross-section of tubular organs. Obtaining a precise cross-section is the critical step to perform quantitative analysis of those organs, for which diameter or area are often correlated to pathologies. Our estimation method, based on a covariance measure from the Voronoi cells of the set of studied points, can be computed either from the skeleton representation, or from the whole set of voxels of the segmented tubular organ. This estimator can give a cross-section estimation from any point of the organ, and is both more accurate and more robust to segmentation errors than state-of-the-art methods.

1 Introduction

The diameter/area estimation of tubular organs such as vessels, airways or colons is of interest since these measurements are often correlated with pathologies. A reliable tool providing, with reproductive results, such geometric characteristics and allowing to study their variations may lead to further progress in health research. One domain which particularly requires such tools is the research on pulmonary diseases. The airway wall thickness is a pertinent indicator correlated with the severity of lung diseases such as asthma [9]. It can be obtained directly on one slice of a CT image [8,12]: an experienced radiologist selects bronchi which appear round on a CT slice and measures them generally by using a dedicated software. This approach is obviously limited as it can only take into account airways which long axes are perpendicular to the image slices. A more advanced approach is based on a segmentation of the airway tree. The segmented volume can be skeletonized so as to obtain its central line. Given a point of the central line and its local direction, it is possible to reconstruct a cross-section of the 3D image which is orthogonal to the airway. Measurements of the airway wall can then be performed in the computed cross-section. A comprehensive airway analysis process following these 4 steps from segmentation to measurements of the airway wall is described in [11].

In this paper, we focus on one step of the analysis process of tubular organs: the computation of accurate cross-sections. This step is hardly described in the existing works although the quality of the final measurements depends on it. It is generally based on the analysis of the skeleton which is supposed to be a curve

skeleton i.e. a 3D digital curve. The main difficulty of computing an orthogonal plane, or equivalently a tangent, to a curve skeleton comes from the irregularities of the curve. A first approach is to smooth the skeleton before computing its tangents as in [11]. The drawback of this approach is that smoothing may not preserve the original object shape. A second approach is to use a 3D digital tangent estimator which captures the exact shape of the 3D curve [10]. It is thus sensitive to the skeleton defects.

We propose a new method to compute accurate orthogonal planes along an unsmoothed skeleton, based on Voronoi Covariance Measure. The covariance measure describes the shape of the Voronoi cells generated by the skeleton points, from which we can deduce the local shape of the object. Furthermore, this measure being defined on any compact, we can apply it either on the set of skeleton points, similarly to existing methods, or on the whole set of points of the segmented object, so it can take into account the full shape of the organ.

In section 2 we present the related works about the estimation of cross-section from a segmented tubular organ, i.e. the skeleton extraction and the 3D tangent estimation. In section 3 we detail the proposed method. Finally we present the results obtained on both synthetic and real data in section 4, with quantitative comparison with other methods.

2 Related works

As was said in the introductory part, the objective of this article is to estimate precisely the cross-sections along a tubular organ. As input data, we suppose to be given a segmentation of the processed organ, i.e. a connected set of points of the 3D digital grid. The usual way to extract cross-sections consists in two steps: (1) skeletonization of the object, (2) estimation of the tangential direction at each point of the skeleton to obtain the normal vectors of the cross-section planes.

There are different definitions of the skeleton of a digital object, depending on the wanted properties. In the case of a tubular organ, a natural representation is a curve-skeleton, i.e. a thin curve of digital points following the centerline of the organ. An efficient way to obtain such a curve-skeleton is to use a thinning algorithm that will "peel" the object until its is reduced to its centerline. However the obtained skeleton always presents defects irrespective of the thinning method used. Small irregularities of the segmented object lead to unwanted small branches and deformations of the skeleton (see figure 1). Small branches can be deleted by a pruning algorithm but the skeleton deformations that are not consistent with the object shape can distort the cross-section computation. In this paper, we use the thinning algorithm presented in [6], because it is robust to noise, produces a connected skeleton and is parameter-free. Some more recent methods providing the same properties have been tested such as filtered euclidean skeletons [2], but they do not provide better results on our specific tubular case (see figure 1).

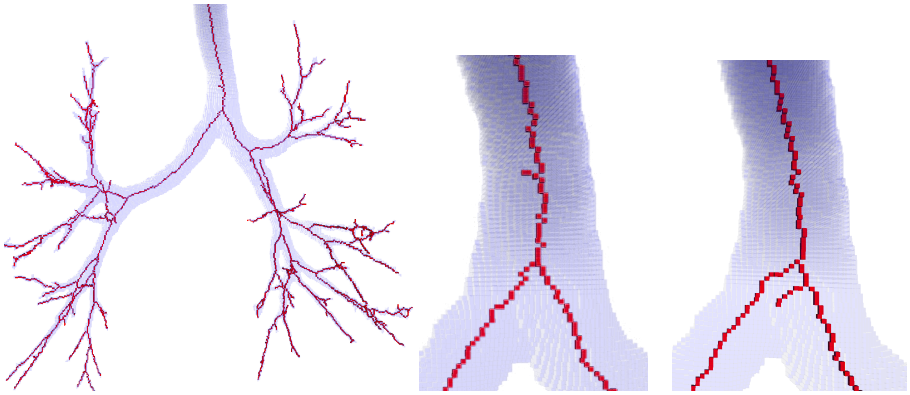

(a) (b) (c)

Fig. 1: (a) Part of a segmented airway-tree and its skeleton. (b) Small irregularities of the segmented object lead to deformations of the curve-skeleton. (c) Euclidean skeleton computed using the method described in [2].

One can define the tangent vector at a point of a 3D digital curve as the vector linking this point and one of its two neighbors on the curve. However, this naive tangent estimation is obviously very sensitive to noise and can not yield accurate results in our context. Other algorithms were designed to better integrate the neighborhood around a point for tangent computation.

Among them the 3D tangent estimator λ-MST recently presented in [10] relies on the recognition of digital straight segments (DSS) along a 3D digital curve. A maximal DSS is a connected subset of the curve corresponding to the digitization of a straight line and which cannot be extended forward or backward. As one point of the curve can belong to several maximal DSS, the main idea is to average the orientations of all the DSS passing through a point in order to compute its tangent (see figure 2).

More precisely, the tangent vector at a given point x is computed as:

$$\boldsymbol{t}(x) = \frac{\sum_{M \in P(x)} \lambda(e_M(x)) \boldsymbol{t}_M}{\sum_{M \in P(x)} \lambda(e_M(x))} \tag{1}$$

where $P(x)$ is the set of maximal DSS passing through x and $\boldsymbol{t}_M$ is the unit direction vector of M. The weights depends on the eccentricity of the point x relatively to the segment M which is defined as $e_M(x) = \dfrac{i_x - m_M}{n_M - m_M}$ where $i_x - m_M$ is the distance as the difference in indices between point x and the last point of M, and $n_M - m_M$ is the DSS length. The function λ is designed to give more weight to the orientation of a DSS if x is close to its center. In our experiments, λ is the triangle function with $\lambda(0) = 0$, $\lambda(1) = 0$ and a peak at 0.5.

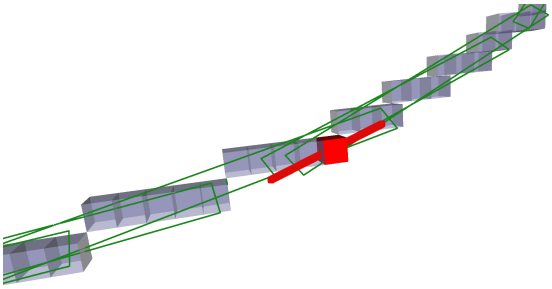

Fig. 2: Computed tangent (red line) at red point on a 3D digital curve. The computed tangent corresponds to a weighted average of the orientations of the digital straight segments (in green) passing through the point.

3 Proposed method

In this article we propose to define a new method to compute precise cross-section for tubular organs, based on the Voronoi Covariance Measure (VCM).

The VCM was first introduced in [7] to estimate normals and curvatures on point clouds sampling a surface. This tensorial measure was shown to be resilient to Hausdorff noise. More recent results proved that it is even robust to outliers [3]. A digital variant of the VCM was defined to analyze digital sets and surfaces [4]. This digital measure was shown to be close to its continuous counterpart and to be efficiently computable. Furthermore its first eigenvector was shown to be multigrid convergent toward the surface normal. It is thus a reliable tool to estimate normals of digital shapes. We propose to develop a cross-section estimator, based on the VCM, that analyse the skeleton of an object. Furthermore we will show that this new tool can also take into account the whole segmented object. Thus the estimator does not only rely on the shape of the skeleton, but can analyze the local shape of the object.

By construction, the VCM computes a covariance matrix of vectors that are aligned with the gradient of the distance to the shape function. Hence, its first eigenvector points toward the normal to the shape (it is the direction that maximizes the distance to the shape when moving along it). Voronoi cells defined by input points tends to align themselves with this gradient. The VCM computes the covariance matrix of all vectors within neighboring cells, hence most of the vectors point in the direction of the shape normal. This is why the VCM robustly estimates the normal direction to the shape.

The VCM was designed to analyse surface sampling, but it can in fact also serve our purpose of finding cross-sections of curve-like shapes. Note that the normal cone of the curve is exactly its cross-section plane. The two first eigendirections of the VCM are not predictable, but they will both try to span the normal cone. Since they are forced to be orthogonal, they will both lie in the cross-section plane.

The digital approximation of the VCM is defined [4] on any point p of a digital set, by considering a neighborhood of p defined by a ball, and summing the covariance measure of the Voronoi cells for which the generator is inside this neighborhood.

Definition of (digital) Voronoi Covariance Measure. Let X be a set of points of the 3D digital grid $\mathbb{Z}^3$. $\Omega_X(R)$ is defined as the set of digital points contained in the R-offset of X, i.e. $\Omega_X(R) = \{x \in \mathbb{Z}^3 | \min_{y \in X} \|y - x\| \leq R\}$ (see figure 3). The Voronoi diagram of X partitions the space into cells. Each cell of this Voronoi diagram contains exactly one point of X, called the *generator* of this cell. We define the *projection* $p_X(z)$ of an arbitrary point $z \in \mathbb{R}^3$, as the generator of the cell which contains z. It follows that any point x of $\Omega_X(R)$ is projected in X through p_X. The point $p_X(x)$ is also the point of X minimizing its distance with x.

Given a point y for which we want to compute the VCM value, we center on y a ball of radius r (denoted by $\mathcal{B}_r(y)$). Then the subset of points considered for the computation consists in all the points at distance no greater than R to X (i.e. $\Omega_X(R)$) the projection of which lies in this ball. Therefore, let $DI_X(y) := \Omega_X(R) \cap p_X^{-1}(X \cap \mathcal{B}_r(y))$ be the domain of integration for point y (orange subset on figure 3, right). The *digital VCM* is then defined as a summation of tensorial products:

$$\mathcal{V}_X(y) = \sum_{x \in DI_X(y)} (x - p_X(x))(x - p_X(x))^t$$

It is also easily seen that we can split the computation per Voronoi cell, as a first pass. Then the VCM for point y is the sum of the VCM of every Voronoi cell which generator lies in the ball of radius r around y. The digital VCM can thus be computed efficiently.

In our context, the Voronoi diagram of the digital skeleton defines a partition of the space into Voronoi cells. Globally, the domain of integration is limited by parameter R, which sets the maximum distance to input data. Points further away are not taken into account. Then, for each point of the skeleton, we sum the covariance measure of neighboring Voronoi cells, which gives a smoothed geometric information of the local shape. The two first eigenvectors of $\mathcal{V}_X(y)$ then give a precise estimation of a basis of the plane that is at most orthogonal to data, hence the cross section for this point.

Parameter setting. Our method has the same two parameters r and R than the original method, which was used to study the geometry of surfaces. In our context, we analyze tubular digital objects coming from medical images. Those parameters are set using *a priori*-knowledge about the studied organ. Parameter r corresponds to how many points must be considered to resemble the local shape of the organ. It is dependent on the resolution of the acquisition and the expected curvature of organs. Parameter R bounds the global domain of integration within Voronoi cells. In our case, since the digital sampling has a regular density, Voronoi cells are thin with almost parallel boundaries. Hence it is not necessary to have a large value of R to get a correct estimation of normal

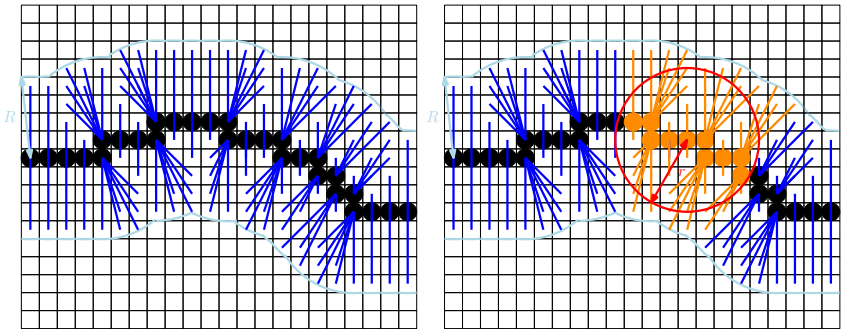

Fig. 3: Left: the limits of the R-offset of a set of digital points are drawn as a cyan contour, while vectors connecting points within the R-offset (i.e. $\Omega_X(R)$) to their projection are drawn in deep blue. Right: Voronoi cells defining the VCM Domain of integration for a kernel of radius r (i.e. $\Omega_X(R) \cap p_X^{-1}(X \cap \mathcal{B}_r(y))$) are drawn in dark orange (both germs and projection vectors). The kernel itself is drawn in red.

directions, and we can expect that a wide range of value for R will give similar results.

Cross-section estimators. In fact, the VCM is generic enough to be applied on an arbitrary set of points. Hence, it can be applied not only to the skeleton of tubular organs, but to the whole tubular organs. We will see in next section that this volumetric approach is even more precise and robust for cross-section estimation along the organs. For any non singular matrix M, we write $\pi(M)$ the plane spanned by its first two eigenvectors (in decreasing order). For a digital set V representing a tubular organ and letting X being the skeleton of V, we thus define our two cross-section estimators as:

1. The *VCM cross-section estimator* is defined for any point $x \in X$ as $\pi(\mathcal{V}_X(x))$.
2. The *Volume VCM cross-section estimator* is defined for any point $x \in X$ as $\pi(\mathcal{V}_V(x))$.

Note that this volumetric approach also approximate cross-section directions because

- the VCM is null on points located inside V, since Voronoi cells are reduced to the point itself,
- and the VCM approaches the normal direction on points located on the boundary of V.

The drawback of the second approach is that we need to know approximately the radius of the studied tubular organs in order to set parameter r consistently. It must be indeed big enough to reach the boundary of V from any point of X. This is not a problem in our context since we know the organ under study.

4 Results

In this section, the VCM efficiency for computing orthogonal planes is compared to the λ-MST method. These methods have been implemented using the DGtal library [1]. We will compare the methods both on synthetic and real data.

4.1 Noisy synthetic data

The goal of this section is to compare our method to the λ-MST estimator on known volumes with altered surfaces. We have generated two different synthetic data sets: a slightly curved cylinder with constant diameter (Figure 4a), and a straight elliptic cylinder with varying minor and major axes values (Figure 7a).

Tubular-like organs are obviously not perfect cylinders, and furthermore the discretization and the segmentation processes will lead to many irregularities on surfaces. These irregularities are the source of skeleton distortions. In order to generate similar irregularities on the synthetic data we have added some noise on the surfaces of the two objects. Noisy versions of the volumes are produced using a simplified version of Kanungo's algorithm [5], implemented in the DGtal library. This method adds noise on binary images by switching the value of each voxel, according to its distance d to the object boundary, with a probability α^d. Cavities and unconnected noisy voxels are then removed using morphological operators.

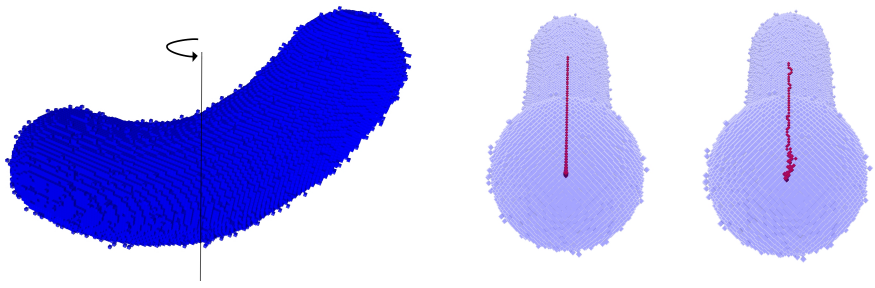

(a) (b) (c)

Fig. 4: (a) Noisy tubular volume generated using a ball with constant radius, disturbed by a Kanungo noise. (b) Volume with the digitized initial centerline used to generate it in red. (c) Computed skeleton showing small distortion compared to the original one.

The first test to assess our method's robustness consists in extracting geometric characteristics on the computed 2D orthogonal planes, and in comparing them to known values. At each point, we used the different methods to compute an orthogonal plane.

The intersection between each orthogonal plane and the unaltered digital curved cylinder should be a disk. In order to quantify how close to a disk the results are, two parameters are computed on the 2D shape resulting from the intersection:

- the area in number of pixels
- the roundness, given by $r = \frac{4A}{\pi * a^2}$ where a is the length of the major axis, and A the area. This value ranges from 0 (line) to 1 (perfect circle).

The corresponding expected values can be computed with the known radius of the cylinder (20 pixels).

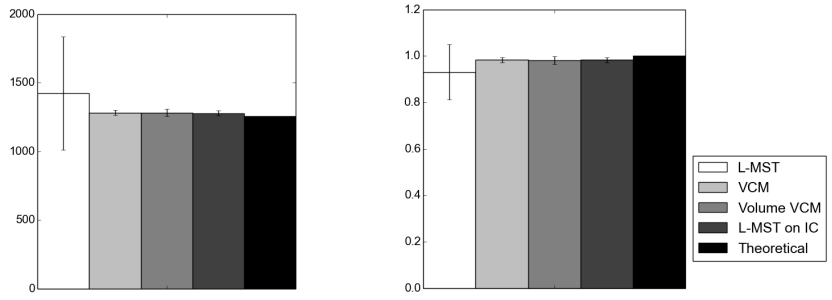

(a) (b)

Fig. 5: (a) Area in pixels and (b) roundness mean values for all the orthogonal planes found in a generated noisy tube volume. The λ-MST on the computed skeleton (white) yields results with high-variability, whereas the λ-MST method applied on the initial centerline and the two VCM methods applied on the computerized skeleton and the volume respectively are consistent with the theoretical values.

The results are obtained on 93 cross-sections. The mean values obtained with the two variants of the VCM method (see figures 5a and 5b), are closer to the theoretical value than those obtained with λ-MST method on the computed skeleton. Furthermore the difference in standard-deviation between the two methods is significative here. The coefficient of variation, defined as the ratio of the standard deviation to the mean, is 29% and 12% for the λ-MST, against 1.5% and 1.1% for the VCM, for the area and roundness respectively. This reflects the high-variability of the λ-MST method, as it finds a substantial number of incorrect orthogonal planes, whereas the results of the proposed method are consistent.

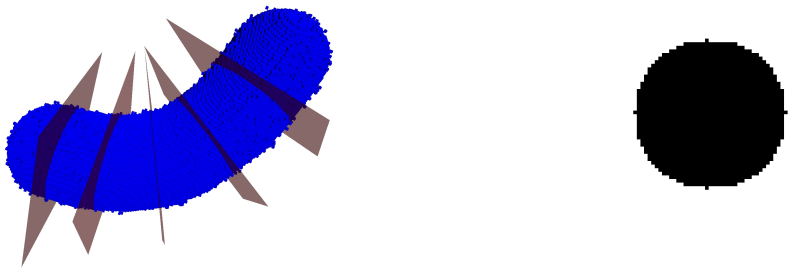

(a) (b)

Fig. 6: (a) Examples of orthogonal planes obtained on a noisy tube-like volume with the volumetric VCM method and (b) typical associated 2D plane.

The second test on synthetic data consists in evaluating the difference between the normal direction of the estimated plane, and the known value. This test has been performed on the straight elliptic cylinder for which the normal direction at each point of its central line is constant. For each point of the skeleton, the angle defect between the computed normal and the expected normal is determined for all methods. Figure 7b shows the results we obtain.

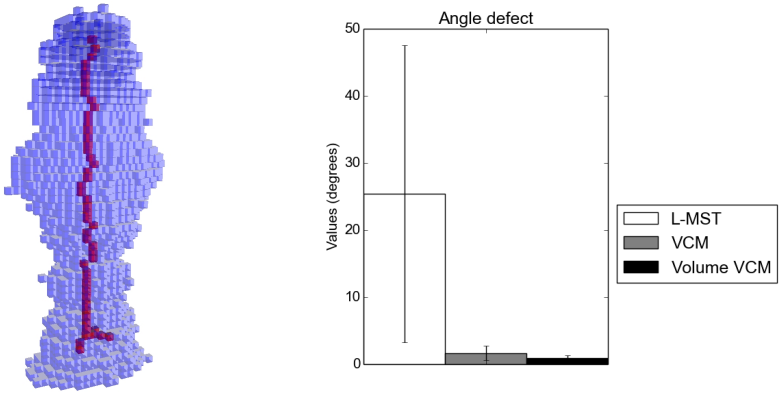

(a) (b)

Fig. 7: (a) Noisy elliptic cynlinder with varying minor and major axes, generated along a centerline with constant normal direction. The computed skeleton is shown in red. (b) The angle defect (in degrees) between the computed normal and the expected normal shows our method outperforms the λ-MST tangent estimator.

The results are obtained on 50 slices. Using VCM on both the skeleton curve and the volume yields an angle defect close to zero, with a low standard deviation. The mean value of the angle defect are greater for the λ-MST, and again suffers from high-variability (standard deviation of 22 degrees against 1.1 and 0.46 degrees for the VCM on the curve and on the volume respectively). The λ-MST estimator does not perform well because DSS recognition is sensitive to slight pixel deviation in a curve: in some cases, short DSS are found which means the computed orientation is not representative of the actual tangent (see figure 8).

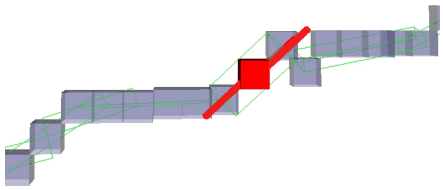

Fig. 8: Altered skeleton leading to short DSS computation and to deviated tangent (red line) at red point.

4.2 Real data

In this section, we present results obtained on a bronchial tree acquired from a CT-scan. The bronchi have been segmented manually, and the skeleton was computed on the resulting volume with the method [6]. Parts of the skeleton are impacted by irregularities of the surface. This leads to some incorrect orthogonal planes estimation with the λ-MST method (see figure 9a) in these parts. On the contrary, similarly as what was observed on synthetic data, the VCM method gives consistent results which are not affected by slight distortions on the skeleton.

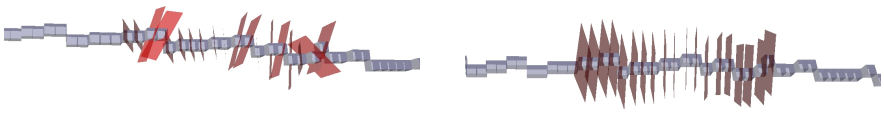

(a) (b)

Fig. 9: Orthogonal planes computed on the skeleton of an airway-tree with (a) λ-MST and (b) VCM. The λ-MST method gives many wrong cross-section directions while the VCM method is consistent all along the path.

We would like to point out that the user must take care on branching parts, since many branches of the skeleton may influence the local computation (see figure 10). However, in practical cases, the orthogonal planes estimation is done branch by branch and thus this influence is low. Furthermore the first planes estimated after a branching part are not of interest since they will not only contain a section from a tubular part, but also a large part of the second beginning branch.

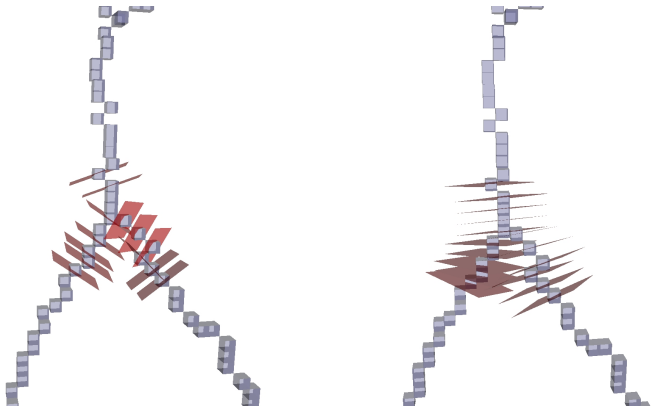

(a) (b)

Fig. 10: Orthogonal planes computed on a branching part of an airway-tree with λ-MST method (a) and our method (b). Without branch separation, it can lead to some misplaced cross-section.

5 Conclusion and Perspectives

We have presented in this article a new reliable method to perform cross-section estimation on tubular organs. We have shown this method performs better than existing ones on the skeleton of the object, and furthermore can be defined to rely on the full shape of the object and thus not be influenced by the irregularities of the skeleton.

This is a method of choice to produce automatic and reproducible quantification of geometrical features from tubular organs, and thus can lead to new advances in health research. Our first application focus on human airways analysis, but it can also be used to study other tubular organs.

Even if the two parameters of our method can easily be set in practice thanks to the *a priori*-knowledge about studied organs, we are currently working to develop a fully automated method. Our automatic settings of those parameters will rely on local geometrical information such as curvature and distance transform (in the volumetric estimation case) to automatically set appropriate radius.

Furthermore we plan to develop a new skeletonization algorithm based on our method. Since it produces orthogonal planes directly from the volume, their centers of gravity can define the skeleton points.

References

1. DGtal: Digital geometry tools and algorithms library, url : http://dgtal.org
2. Couprie, M., Coeurjolly, D., Zrour, R.: Discrete bisector function and Euclidean skeleton in 2D and 3D. Image and Vision Computing 25(10) (Oct 2007)
3. Cuel, L., Lachaud, J.O., Mérigot, Q., Thibert, B.: Robust geometry estimation using the generalized voronoi covariance measure. arXiv preprint arXiv:1408.6210 (2014)
4. Cuel, L., Lachaud, J.O., Thibert, B.: Voronoi-based geometry estimator for 3d digital surfaces. In: Discrete Geometry for Computer Imagery. pp. 134–149. Springer (2014)
5. Kanungo, T., Haralick, R., Baird, H., et al.: A statistical, nonparametric methodology for document degradation model validation. IEEE Trans. Pattern Anal. Mach. Intell. 22(11), 1209–1223 (2000)
6. Lee, T.C., Kashyap, R.L., Chu, C.N.: Building skeleton models via 3-d medial surface/axis thinning algorithms. CVGIP: Graph. Models Image Process. 56(6), 462–478 (1994)
7. Mérigot, Q., Ovsjanikov, M., Guibas, L.: Voronoi-based curvature and feature estimation from point clouds. Visualization and Computer Graphics, IEEE Transactions on 17(6), 743–756 (2011)
8. Orlandi, I., Moroni, C., Camiciottoli, G., et al.: Chronic obstructive pulmonary disease: Thin-section ct measurement of airway wall thickness and lung attenuation 1. Radiology 234(2), 604–610 (2005)
9. Pare, P., Nagano, T., Coxson, H.: Airway imaging in disease: Gimmick or useful tool? Journal of Applied Physiology 113(4), 636–646 (2012)
10. Postolski, M., Janaszewski, M., Kenmochi, Y., Lachaud, J.O.: Tangent estimation along 3d digital curves. In: ICPR. pp. 2079–2082 (2012)
11. Tschirren, J., Hoffman, E.A., McLennan, G., Sonka, M.: Intrathoracic airway trees: segmentation and airway morphology analysis from low-dose ct scans. Medical Imaging, IEEE Transactions on 24(12), 1529–1539 (2005)
12. Yamashiro, T., Matsuoka, S., Estépar, R.S.J.: Quantitative assessment of bronchial wall attenuation with thin-section ct: an indicator of airflow limitation in chronic obstructive pulmonary disease. American Journal of Roentgenology 195(2), 363–369 (2010)